

# MICRO SOLID OXIDE FUEL CELLS WITH PEROVSKITE-TYPE PROTON CONDUCTIVE ELECTROLYTES

Hiroo Yugami <sup>1\*</sup>, Kensuke Kubota <sup>1</sup>, Fumitada Iguchi <sup>1</sup>, Shuji Tanaka <sup>1</sup>, Noriko Sata <sup>1</sup> and Masayoshi Esashi <sup>2</sup>

<sup>1</sup> Graduate school of engineering, Tohoku University, Sendai, Japan

<sup>2</sup> World Premier International Research Center Advanced Institute for Materials Research, Tohoku University, Sendai, Japan

\*Presenting Author: h\_yugami@energy.mech.tohoku.ac.jp

**Abstract:** This paper reports the adoption of new electrolytes to micro solid oxide fuel cells ( $\mu$ -SOFC) fabricated using silicon MEMS fabrication technology. The new electrolytes, *i.e.* yttrium doped BaZrO<sub>3</sub> and strontium doped LaScO<sub>3</sub>, are perovskite type proton conductors and will enable  $\mu$ -SOFC to work at the temperatures lower than 400°C, because those electrolytes show significantly higher electrical conductivity than conventional oxygen ionic conductors. We fabricated  $\mu$ -SOFC with those electrolytes and evaluated the performance. The results indicate that  $\mu$ -SOFC can work during the temperature range of 300°C to 400°C, although the improvement of the performance is essentially required.

**Keywords:** micro solid oxide fuel cells ( $\mu$ -SOFC), perovskite type proton conductors, yttrium doped BaZrO<sub>3</sub> (BZY), strontium doped LaScO<sub>3</sub> (LSSc)

## INTRODUCTION

Micro solid oxide fuel cells ( $\mu$ -SOFC) fabricated using silicon MEMS fabrication technology are new application of SOFC, which usually developed for the domestic co-generation system and the replacement of a thermal power plant. SOFC can generate electricity at high power density and high efficiency. In addition, the liquid fuels of SOFC such as methanol, butane and liquid propane gas, have high energy density over 10MJ / kg (HHV). Those benefits make  $\mu$ -SOFC more attractive for the power sources of mobile electric devices.

Reported power density of  $\mu$ -SOFC, 861mW /cm<sup>2</sup> at 450°C [1] and 150mW / cm<sup>2</sup> [2], is quite promising. But, the improvement of mechanical stability and operation much lower than 400°C are essential problems to be solved for practical application. Lowest operating temperature is determined by the area specific resistance of  $\mu$ -SOFC, and the resistance strongly depends on the component materials and geometrical structure. Almost developed  $\mu$ -SOFC have used yttria stabilized zirconia (YSZ) as an electrolyte, and it is used for conventional SOFC operated higher than 750°C. Considering electrical conductivity at the temperature lower than 400°C, it is not suitable. So, the replacement of an electrolyte will directly beneficial to reduce operating temperature.

In this study, we developed  $\mu$ -SOFC with new electrolytes, and evaluated cell performances of them. As electrolytes, we adopted perovskite type proton conductors, *i.e.* yttrium doped BaZrO<sub>3</sub> and strontium doped LaScO<sub>3</sub>. Those have been developed for intermediate temperature operating, *i.e.* 700°C-400°C, SOFC, and show higher electrical conductivity than YSZ over two orders of magnitude [3, 4].

## EXPERIMENTAL

In this study,  $\mu$ -SOFC was fabricated on (100) oriented silicon wafers. Detailed design was shown in Fig.1. Each silicon wafers have 16 cells and the cell size is in the range of  $\square$ 300 $\mu$ m to  $\square$ 600 $\mu$ m. SiO<sub>2</sub> insulation layers were thermally created on the both sides of the silicon wafers and used as substrates. Thin electrolyte films ( $t \approx 200$ nm) of 20mol% Sr-doped LaScO<sub>3</sub> (LSSc) or 15mol% Y-doped BaZrO<sub>3</sub> (BZY) were deposited on the SiO<sub>2</sub> surface using conventional pulsed laser deposition (PLD) method. Previously, we found that residual stress could be controlled by oxygen partial pressure during PLD process [5]. So, we controlled oxygen partial pressure at 1Pa to keep residual stress little compressive to prevent the brittle and buckling fracture of the electrolyte.

Anode gas chamber was penetrated as a trapezoid shape by wet anisotropic etching using TMAH, and finished by XeF<sub>2</sub> etching. After the penetration, Pt-Pd porous electrodes were sputtered on the both sides of the electrolyte as anode and cathode. The thickness of porous electrode was about 100nm.

To evaluate cell performances, we performed power generation test and electrical impedance measurement using an instrument shown in Fig.2. A sourcemeter (Keithley, type 2400) and the combination of a dielectric interface (Solartron, SI1296) and a frequency response analyzer (Solartron, SI1260) were used for those tests.

The silicon wafer with  $\mu$ -SOFC was located on the stage and sealed by aluminum cement to the stage. Ring shape external heater heated the silicon wafer and the stage up to 400°C. Anode and cathode atmospheres were humidified (20°C) hydrogen and laboratory air.

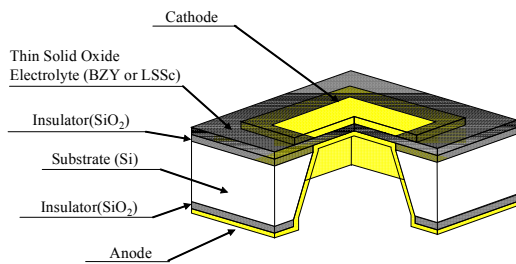


Figure 1 schematic illustration of  $\mu$ -SOFC.

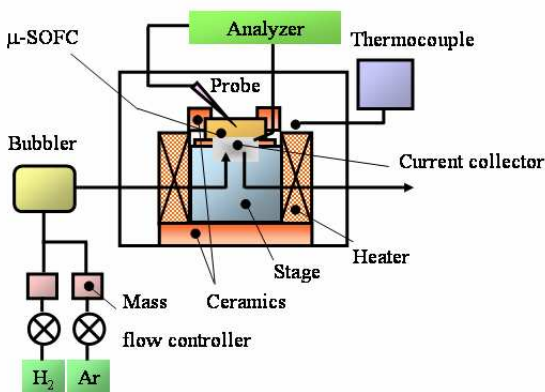


Figure 2 schematic diagram of an instrument for the evaluation of cell performances.

## RESULTS AND DISCUSSION

Residual stress in BZY and LSSc thin electrolytes is confirmed to be little compressive and the value is confirmed in the range of 0.5GPa to 1GPa by XRD. Those compressive stress concaves and folds the electrolytes just after penetration of the substrate by the etching as shown in Fig.3. The profile of concaved BZY electrolyte can be fitted by circular arc and the length of indicates that the increment of length is 1% at maximum. This expansion well correlates with the value of the residual stress.

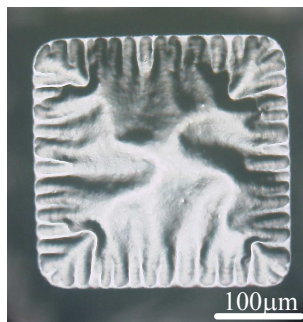


Figure 3 optical image of  $\mu$ -SOFC with BZY electrolyte.

Residual stress controlling is beneficial to improve yields in manufacturing process. The yields rate of 16

cells on the same silicon wafer are approximately 100%, and we can obtain the cells with the size up to  $\square 600\mu\text{m}$ . Residual stress controlling also improves thermal stability. Fabricated  $\mu$ -SOFC withstands several thermal cycles, if heating and cooling rates are limited lower than  $120^\circ\text{C}/\text{h}$ . However, concaved electrolyte plastically deforms to be flat by thermal cycles as shown in Fig.4. This flattening decreases resistivity to thermal cycles. So, this phenomenon should be prevented or suppressed in future.

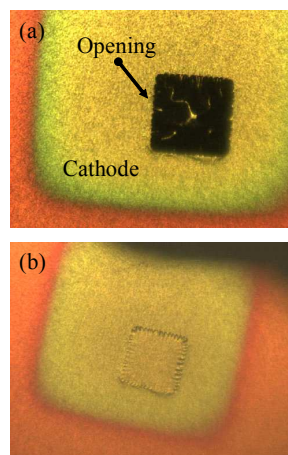


Figure 4 Optical images (a) before and (b) after thermal cycle.

Figure 5 shows typical impedance spectrum of a cell at  $300^\circ\text{C}$ . This spectrum consists of several components, and all of the components show Arrhenius type temperature dependence. Those are typical impedance spectrum of SOFC. So, it is confirmed that short circuit between anode and cathode due to the defect of the BZY electrolyte does not occur and a cell is successfully fabricated on the substrate.

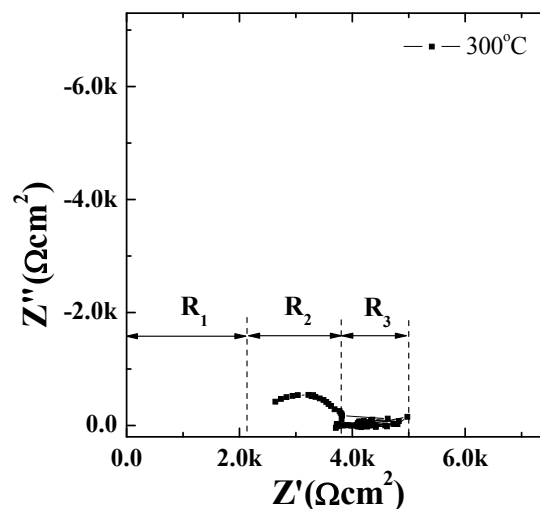


Figure 5 typical impedance spectrum at  $300^\circ\text{C}$  of a  $\mu$ -SOFC with a BZY electrolyte.

Total cell resistance is about  $5k\Omega\text{cm}^2$ , and the

value is quite large for the purpose of  $\mu$ -SOFC, although 300°C increases total cell resistance. The value indicates that maximum current is in the range of several hundreds  $\mu\text{A}/\text{cm}^2$  lower than by three orders magnitude than reported values. So, it is essential to improve total cell resistance drastically.

Considering relationship between those components ( $R_1$ ,  $R_2$  and  $R_3$ ) and the actual resistance of the cell,  $R_1$  at high frequency side, both  $R_2$  and  $R_3$  at low frequency side are generally assigned to be electrolyte resistance and electrode overpotentials, respectively. Comparing those resistance and overpotentials, it is remarkable that all of them are in the same range. In general, electrolyte resistance at such low temperature is quite lower than the overpotentials of electrolyte [6]. But, in this case, calculated electrolyte resistivity is about  $10^8 \Omega\text{cm}$ . By contrast, the resistivity of BZY in the literature is  $100\Omega\text{cm}$ . The difference is over the five orders of magnitude. The reason why is not clear yet, but it is one problem of the cell to be improved. For electrode overpotentials, those values do not defer from the literature values using porous Pt electrodes [7]. This indicates that the potential of Pt-Pd porous electrodes is limited, and it is suggested that electrodes should be improved by the adoption of other promising materials. Because it is well known that mixed ionic and electronic conductors and small amount of FeO and Pd catalysts are beneficial for cathode and anode in low temperature operation, respectively [8], the adoption of electrodes based on those materials will improve electrodes overpotential.

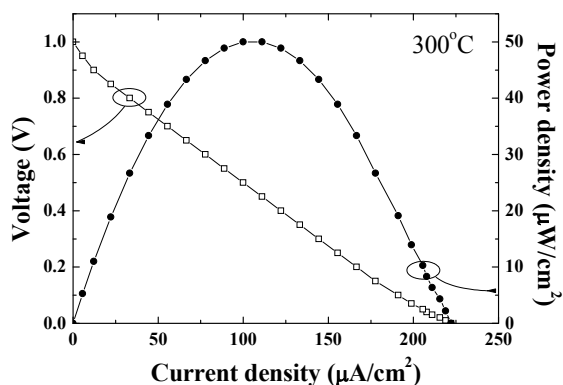


Figure 6 I-V and I-P characteristics at 300°C.

Figure 6 shows the results of power generation test. In this test, we obtain open circuit voltage (OCV) at 0.98 V using the cell configuration of humidified (20°C)  $\text{H}_2$  | Pt-Pd | BZY | Pt-Pd | laboratory air. On the assumption that the humidity of laboratory air is 50% at 25°C, theoretical OCV at 300°C is 1.198V. Because physical leakage of fuel or air to opposite side causes more significant OCV drop, this result proves the gas tightness of the cell. Hence, observed OCV drop from theoretical value is supposed to be due to internal short circuits in the electrolyte. However, in the literature,

the OCV drop by internal short circuits was not expected at 300°C. So, detailed analysis of electrolyte properties focused on huge resistivity and unexpected short circuits should be necessary.

I-V and I-P characteristics are well corresponded to the impedance spectrum and OCV. From the impedance spectrum, total cell resistance is estimated to be  $5\text{k}\Omega\text{cm}^2$ . Hence, maximum current is calculated to be about  $200\mu\text{A}/\text{cm}^2$ , and observed short circuit current is  $222\mu\text{A}/\text{cm}^2$ . This result also indicates that the improvement of total resistance is quite important.

However, we can obtain OCV over 0.9V at the temperature over 300°C as shown in Fig. 7. This reveals that fabricated  $\mu$ -SOFC can work at the temperature lower than 400°C.

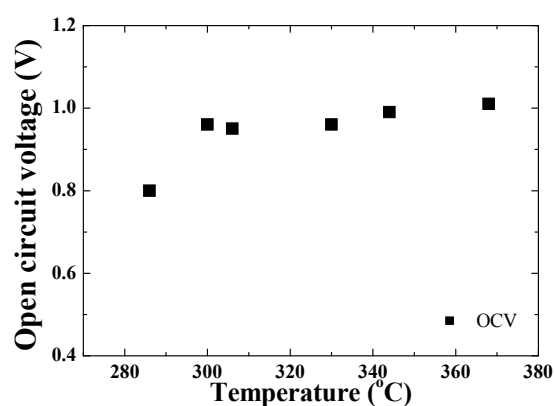


Figure 7 Open circuit voltage as a function of temperature.

## CONCLUSION

In this study, we adopted perovskite type proton conductors of BZY and LSSc as electrolytes of  $\mu$ -SOFC, and evaluated cell performance at the temperature lower than 400°C. We successfully fabricated the  $\mu$ -SOFC with BZY and LSSc on the silicon wafer at high yield rate, and fabricated cell with BZY was proved to work in the temperature range of 300°C to 400°C. But, the cell showed quite high total resistance and low performances. Hence, we confirmed the importance of total resistance is essential for the development of  $\mu$ -SOFC.

## ACKNOWLEDGEMENT

This study was performed in R&D Center of Excellence of Integrated Microsystems, Tohoku University under the program “Formation of Innovation Center for Fusion of Advanced Technologies” supported by Special Coordination Funds for Promoting Science and Technology.

## REFERENCES

- [1] Su, P.-C., Chao, C.-C., Shim, J. H., Fasching, R., and Prinz, F. B., *Nano Letters*, **8**(8), pp. 2289-2292.

- [2] Bieberle-Hutter, A. *et al.*, *Journal of Power Sources*, **177**(1), pp. 123-130.
- [3] Iguchi, F., Sata, N., Tsurui, T., and Yugami, H., *Solid State Ionics*, **178**(7-10), pp. 691-695.
- [4] Kato, H., Kudo, T., Naito, H., and Yugami, H., *Solid State Ionics*, **159**(3,4), pp. 217-222.
- [5] Takahashi, T., Iguchi, F., Yugami, H., Esashi, M., and Tanaka, S., *Nippon Kikai Gakkai Ronbunshu, B-hen*, **75**(751), pp. 524-526.
- [6] Iguchi, F., Tokikawa, T., Miyoshi, T., Tsurui, T., Nagao, Y., Sata, N., and Yugami, H., *ECS Transactions*, *7(1, Solid Oxide Fuel Cells 10 (SOFC-X), Part 2)*, pp. 2331-2336.
- [7] Iguchi, F., Nagai, M., Sata, N., and Yugami, H., *ECS Transactions*, *25(2, Solid Oxide Fuel Cells 11 (SOFC-XI))*, pp. 1759-1766.
  
- [8] Hibino, T., Hashimoto, A., Suzuki, M., and Sano, M., *Journal of the Electrochemical Society*, **149**(11), pp. A1503-A1508.